PCCP

RSC Publishing

COMMUNICATION

View Article Online
View Journal | View Issue

Cite this: *Phys. Chem. Chem. Phys.*, 2013, **15**, 3433

Received 8th December 2012,
Accepted 15th January 2013

DOI: 10.1039/c3cp44415e

www.rsc.org/pccp

Orientation selection in distance measurements between nitroxide spin labels at 94 GHz EPR with variable dual frequency irradiation†

Igor Tkach,[a] Soraya Pornsuwan,[a] Claudia Höbartner,[b] Falk Wachowius,[b] Snorri Th. Sigurdsson,[c] Tatiana Y. Baranova,[d] Ulf Diederichsen,[d] Giuseppe Sicoli[a] and Marina Bennati*[ad]

Pulsed electron–electron double resonance (PELDOR, also known as DEER) has become a method of choice to measure distances in biomolecules. In this work we show how the performance of the method can be improved at high EPR frequencies (94 GHz) using variable dual frequency irradiation in a dual mode cavity in order to obtain enhanced resolution toward orientation selection. Dipolar evolution traces of a representative RNA duplex and an α-helical peptide were analysed in terms of possible bi-radical structures by considering the inherent ambiguity of symmetry-related solutions.

Measurements of inter-spin distances on the nanometer scale by pulsed electron paramagnetic resonance (EPR) spectroscopy have become a frequently used spectroscopic tool to gain structural information about proteins or nucleic acids. The experiment[1–4] requires either endogenous paramagnetic centers or the insertion of spin labels by site specific modifications of the investigated biomacromolecule.[5] This technique can also provide information on the relative orientation of the spin probes,[6] if they are oriented in the biomolecule under study, as in the case of endogenous amino acid radicals and co-factors[7,10] or nitroxide radicals in nucleic acids.[8] Nevertheless, general applicability of the orientation measurements using nitroxide spin labels in diamagnetic proteins, in spite of their extensive application as distance markers, is still representing a challenge. This is not only due to the variety of possible conformations that some labels can adopt within the bio-macromolecule, but moreover, to the difficulties related to the performance of a two frequency pump–probe pulsed EPR experiment in the millimeter-wave range, as discussed in several recent papers.[7,9–15] This bottleneck has prevented an extended examination of orientation selection at high frequencies in contrast to the method at low EPR frequencies (9 GHz).[16–19] Particularly, recent analysis of orientation selection at low frequencies revealed that the problem of reconstructing bi-radical structures based on triples of Euler angles is non-trivial due to ambiguities in the solutions.[18] In the present work, we demonstrate the performance of 94 GHz PELDOR/DEER by employing a novel dual-mode resonator[20] in the millimeter-wave range that covers all possible frequency separations in the EPR spectrum of spin labels and is adapted to a commercial spectrometer. The results permit us to explore the feasibility of data analysis for two representative cases of biological systems, a RNA duplex and an α-helical peptide. We employ spin labels with restricted mobility, which substantially simplify data analysis of possible conformational distributions.[21–23] The chemical structure of the spin labels as well as their insertion position in the respective sequences is displayed in Fig. 1. Synthesis and characterization of the samples were described in previous papers.[22,23]

The experiments were based on the 4-pulse DEER (double-electron electron resonance) or PELDOR (pulsed-electron double resonance) sequence to measure inter-spin distances that requires two microwave frequencies to pump and detect each electron spin of the target bi-radical, respectively. The distance information is encoded in the observed dipolar oscillation and can be best determined in experiments at low EPR frequencies (9 GHz/0.34 T). The time evolution of the echo intensity for an isolated spin pair AB is given by:[1,2]

$$V(t) = V_0(1 - \lambda(1 - \cos(\omega_d(1 - 3\cos^2\theta_{dd})t))) \quad (1)$$

where V_0 is the echo intensity at the time $t = 0$, θ_{dd} is the angle between the dipolar vector and the external magnetic field, λ is the modulation depth or the fraction of spin pairs excited by

[a] *Research Group EPR Spectroscopy, Max Planck Institute for Biophysical Chemistry, Am Fassberg 11, 37077 Göttingen, Germany. E-mail: marina.bennati@mpibpc.mpg.de; Fax: +49 551 201 1383; Tel: +49 551 201 1911*

[b] *Research Group Nucleic Acid Chemistry, Max Planck Institute for Biophysical Chemistry, Am Fassberg 11, 37077 Göttingen, Germany*

[c] *University of Iceland, Department of Chemistry, Science Institute, Dunhaga 3, Reykjavik, Iceland*

[d] *Institute of Organic and Biomolecular Chemistry, Georg-August University of Göttingen, Tammannstr. 2, Göttingen, Germany*

† Electronic supplementary information (ESI) available: X-band data, details of the data analysis, plots of symmetry related solutions. See DOI: 10.1039/c3cp44415e

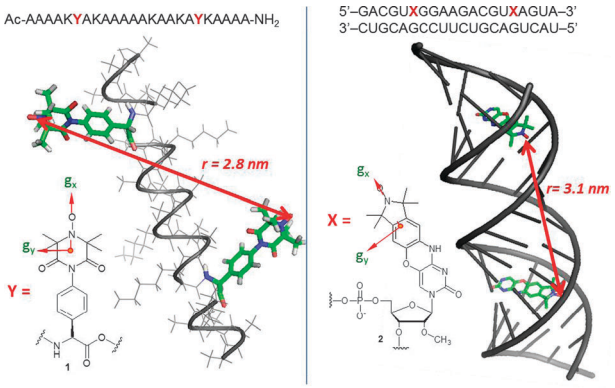

Fig. 1 Schematic structures (PyMol, DeLano Scientific LLC) of the investigated biomolecules, *i.e.* an α-helical peptide (left) and a RNA duplex (right) containing nitroxide spin-labels with restricted mobility. The orientation of the magnetic ***g***-tensor in the nitroxide radicals is illustrated. Inter-spin distances of 3.1 ± 0.3 and 2.8 ± 0.2 nm were determined at 9 GHz (Fig. S1 and S2, ESI†). Previous studies indicated that insertion of the spin labels does not affect the standard A-form of the RNA duplex as well as the α-helical peptide structure.[22,23]

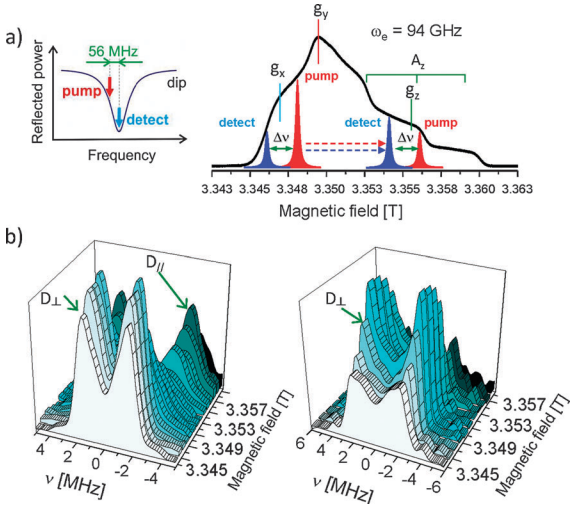

Fig. 2 94 GHz DEER/PELDOR at a fixed frequency separation of 56 MHz. (a) 94 GHz ESE spectrum of the RNA sample showing the pulse excitation width and the band width limitation of a single mode cavity (left). (b) FT-dipolar spectra for the RNA (left) and the α-helical peptide (right) as a function of the observation field. Maximum λ was 5% for the RNA and 4.5% for the peptide. Intensities are scaled with respect to λ_{max}. The number of traces was selected based on the field steps with size on the order of the excitation band width (~10 G). Exp. parameters: [C] = 60 μM (RNA) and 50 μM (peptide), $\pi/2$ = 16 ns, π = 32 ns, π_{ELDOR} = 56 ns, $\Delta\nu$ (fixed) = 56 MHz, shots per point (SPP) = 20, shot repetition time (SRT) = 10 ms, 2-step phase cycling, 36–196 scans (1.3–7 h). T = 50 K.

pump and detection pulses. The dipolar frequency ω_d of an isolated spin pair AB is related to the inter-spin distance r_{AB} by:

$$\omega_d = \frac{\mu_0 \mu_B{}^2 g_A g_B}{4\pi\hbar r_{AB}{}^3} \quad (2)$$

g_A and g_B being the g values of the two spins. If the modulation depth does not depend on the molecular orientation, $V(t)$ results from the sum of contributions of all possible orientations θ_{dd}. When the experiment is performed at so-called high field and frequency, *i.e.* $\omega_e \geq$ 94 GHz, the EPR line of nitroxides is dominated by the anisotropy of the electron Zeeman interaction (***g*** anisotropy). In this case, if orientation correlation between the labels exists, the DEER/PELDOR traces $V(t)$ become a function of the mutual radical orientation. First, the distribution of the dipolar frequencies in the traces depends on the fraction of detected molecular orientations. Second, the modulation depth reflects the probability for a concomitant excitation of radicals belonging to a given pair.[6–9] The Fourier Transformation (FT) of the traces results in distorted dipolar Pake patterns (*i.e.* incomplete distribution of dipolar frequencies in a powder sample) with characteristic line intensities given by the afore-mentioned probability function.

In Fig. 2 we display a series of 94 GHz DEER/PELDOR experiments of the RNA duplex and the α-helical peptide. A commercial W-band resonator (Bruker TeraFlex) was used that allows for a maximal separation of pump and detection frequencies of 56 MHz at 400 mW of available microwave power (Bruker Power Upgrade 2).[12] For the RNA duplex (Fig. 2b, left), the orientation selection at 94 GHz shows clear deformations of the Pake patterns, with the parallel component of the dipolar tensor ($D_\parallel$) appearing at resonances close to g_z in the EPR spectrum and maximal modulation depth observed between g_x and g_y. This is qualitatively consistent with a distance vector interconnecting the labels that is almost parallel to the duplex stacking axis (Fig. 1). We note that the observation of such a pronounced orientation effect in the RNA sample is made possible by the well-defined orientation of the label, as found by a comparative experiment with a more flexible TEMPO-derived label;[24] in the latter experiment we were not able to observe any orientation selectivity in the 94 GHz traces. Restricted mobility of the RNA label (Fig. 1) is consistent with a recent crystal structure of an A-form DNA duplex containing this probe[25] and corresponding PELDOR experiments on DNA.[8,13] In contrast, for the α-helical peptide the parallel frequency component of the dipolar tensor is not visible (Fig. 2b, right) but we detect a pronounced field dependence of the peak intensities resulting from a variation in modulation depth in the time traces. We also note that comparative experiments at X-band (9 GHz) display orientation selection in the RNA sample, as previously reported also in DNA sequences,[8,13] but the absence of any orientation effect in the peptide sample (Fig. S1 and S2, ESI†).

In order to better detect orientational selectivity, we performed a second series of experiments by using the dual-mode resonator[20] that permits a frequency separation up to 800 MHz (Fig. 3a). The separation $\Delta\nu$ of pump and detection frequencies was tuned over the entire range of the nitroxide spectrum, *i.e.* up to about 400 MHz (Fig. 3). This procedure is mandatory if the two labels in the bi-radical are non-collinear and their resonances cannot be pumped and detected simultaneously by a small $\Delta\nu$. The experiment with the RNA duplex (Fig. 3b) shows similar results as in Fig. 2b, *i.e.* both frequency components of the dipolar tensor are detectable by changing the detection position in the EPR line. Thus, the data with the two different setups were consistent. In Fig. 3c the dipolar spectra of the α-helical peptide are displayed for various frequency separations across the EPR line. Here, the changes in the Pake patterns become more subtle because of a complex probability response function reflected in the traces. Moreover, the two canonical frequencies of the Pake ($D_\parallel$ and $D_\perp$)

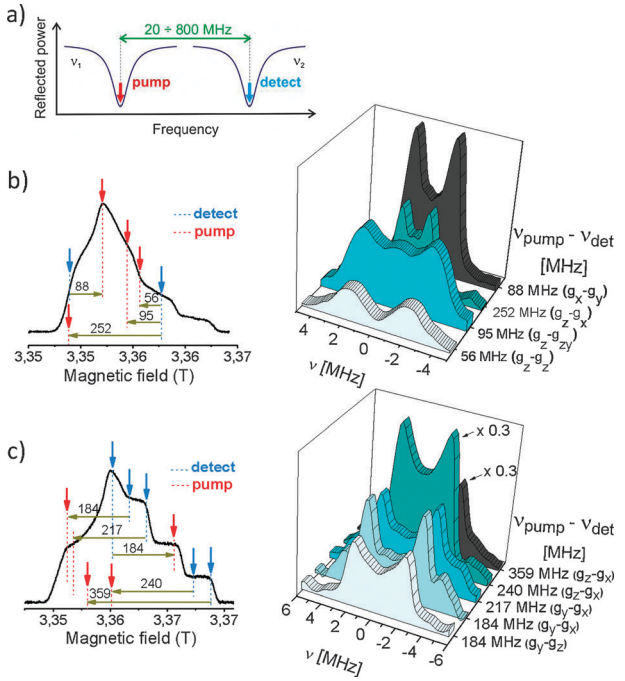

Fig. 3 94 GHz DEER/PELDOR experiments performed at variable frequency separation. (a) Adjustable band width provided by our dual-mode cavity. (b) FT-Dipolar spectra of the RNA and (c) of the α-helical peptide recorded by tuning the frequency separation $\nu_{det} - \nu_{pump}$. (left). Maximum λ was 10% for the RNA and 7% for the peptide. Intensities are scaled with respect to λ_{max}. Pulse lengths were calibrated by spin echo nutations. The total number of traces was selected similar to the experiments in Fig. 2. Exp. parameters: [*C*] = 60 μM (RNA) and 50 μM (peptide), $\Delta\nu_{pump-detect}$ = 56–363 MHz, $\pi/2$ = 28–36 ns, π = 56–72 ns, π_{ELDOR} = 80–88 ns, SPP = 20, SRT = 10 ms, scans = 28–110 (RNA) and 36–128 (peptide). Acquisition time/trace (2-step phase cycling) = 1–4 h (RNA) and 1.3–4.6 h (peptide). *T* = 50 K.

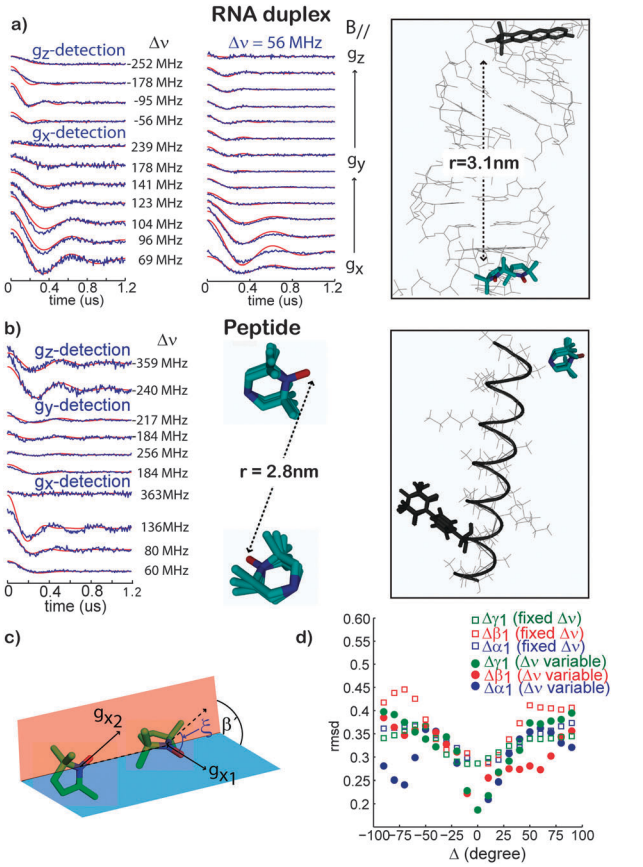

Fig. 4 Left: Comparison of the experimental PELDOR/DEER traces (blue lines) with calculated traces (best fits, red lines) for the experiments at variable and fixed frequency separation of the RNA duplex (a) and for the helical peptide (b), respectively. Center/right: bi-radical structures representing the symmetry-related solutions in Table 1. For the RNA, both data sets deliver similar solutions. For the peptide, only solutions from variable $\Delta\nu$ are considered. (c) Angles between the nitroxide planes, β′, and between the nitroxide N–O bonds, ξ. (d) A representative plot of the rmsd as a function of the variation of the Euler angles α_1, β_1, γ_1 for the peptide.

cannot be separated at any resonance position, suggesting a non-collinear mutual orientation of the ***g*** tensor axes in the bi-radical. More traces at variable frequency separation for both samples are displayed in Fig. 4.

The time traces at 94 GHz with either fixed or variable frequency separations were analyzed independently using home-written fitting routines[7] in MATLAB adapted for nitroxide radicals (ESI†) and the solutions were subsequently compared. The bi-radical structure was defined as the orientation of the spin labels with respect to the common interconnecting dipolar vector. This results in two consecutive Euler rotations, first between the ***g*** frame of spin 2 (either A or B in eqn (2)) into the principal axis of the dipolar tensor ***D*** ($R(\alpha_2, \beta_2, \gamma_2)$) and then from the latter into the ***g*** frame of spin 1 ($R(\alpha_1, \beta_1, \gamma_1)$).[7] Due to the axial symmetry of the ***D*** tensor only five Euler angles are required, therefore the Euler angle γ_2 was set to zero. We point out that both consecutive rotations are required to reconstruct a 3-dimensional bi-radical structure and not only the frame transformation between the ***g*** tensors, which is the product of those. Conformational distribution was neglected for the RNA sample due to the rigid fusion of the nitroxide-containing isoindoline ring to the cytidine nucleobase (Fig. 1) and projecting into the major groove of the RNA duplex.[23] For the TOPP label in the peptide, the nitroxide bond is located at a defined position in space as an elongation of the C_α–C_β axis (Fig. 1), however it possesses one axis of rotation (C_α–C_β) that is almost collinear with the N–O direction.[22] A second rotation is possible around the C–N bond interconnecting the rings, which coincides with the C_α–C_β axis. The combined effect of these two rotations was considered in the analysis through a libration around the N–O (g_x) axis by an angle ψ. The transformations used are illustrated in Scheme 1.

All principal values of the ***g***, ***D*** and hyperfine ***A*** tensors were determined independently from simulations of 94 GHz EPR spectra (Table 1, caption) and distance measurements at 9 GHz (ESI†). To optimize computational time, the parameter ψ for the TOPP label was first set to zero and the obtained best solutions were examined subsequently as a function of ψ. Thus, the parameter space for the fit reduced to five Euler angles defining the bi-radical structure. We tested arbitrary starting sets of Euler angles and the solution mostly converged to the same quintuplet within a distribution of values up to about ±10°. However, from some starting points we found that other combinations of the five Euler angles delivered

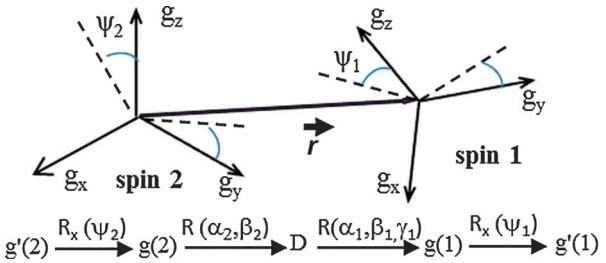

Scheme 1 Frame transformations in a bi-radical structure. ***g*** and ***D*** denote the frames of the ***g***- and the dipolar tensor, respectively. For the TOPP label the angle ψ accounts for a distribution of orientations around the g_x axis up to a value $\pm\psi$ with the angles ψ_1 and ψ_2 taken as one single parameter.

similar fit qualities. A closer inspection of these solutions revealed that they were symmetry-related, as discussed below. In Table 1 we report the solutions from the fits together with derived symmetry-related solutions compatible with the biomolecule structure. The parameters ξ and β' are introduced to describe the angles between the N–O axes of the labels and the nitroxide planes, respectively (Fig. 4c). The libration angle ψ was found to deteriorate the rmsd for values above $\pm20^\circ$ but not to improve it (Fig. S4, ESI†). Consideration of small distributions of the Euler angles would likely improve the analysis but is neglected for simplicity. Time traces superimposed to the obtained fits are displayed in Fig. 4.

Comparison of the entries in Table 1 indicates that in the RNA case the solution from variable $\Delta\nu$ leads to comparable rmsd and ξ, β' angles as the solution for fixed $\Delta\nu$. This is consistent with the fact that the experiment with a small and fixed $\Delta\nu$ is suited for detecting bi-radicals with almost collinear orientations of the labels, as expected in the RNA duplex. On the other hand, the results for the α-helical peptide clearly indicated that the data with variable frequency separation lead to a better quality of fits. This is even more evident when screening the rmsd over the variation of each angle around the solution (Fig. 4d and Fig. S5, ESI†). The rmsd from the data with fixed frequency separation is similar over a wide range of Euler angles, in contrast to well-pronounced minimum observed from the data at variable $\Delta\nu$. This behavior reflects the different capability of the data to pose constraints for the fit.

The result that very different quintuplets of Euler angles delivered very similar rmsd raised the question as to which solution represents the bi-radical structure of the bio-molecule. Ambiguities in the solution were pointed out also in previous works[6,18,27] and are inherent to the symmetry of the spin Hamiltonian involved. Therefore, we examined whether the dipolar traces are sensitive to a change in the directions of the ***g***-tensor principal axes from positive to negative, or, in other words, to a 180° rotation of the spin label around one of the *g* principal axes. Such operations change the quintuplet of Euler angles describing the bi-radical structure and, if applied for instance to label 2, will change the location of label 1 in the 3D space. Thus, we applied all these possible operations (180° rotations around the *g* axes) to the first and second label and also to their combination and arrived at 16 symmetry-related solutions that are listed in the ESI† (Table S6, ESI†). Explicit computation of the traces for all these solutions gave identical fits (rmsd) of the PELDOR traces. Since the labels employed in this study are not distinguishable, the solutions might represent a transformation from label 1 to 2 or *vice versa*.

The 16 symmetry-related solutions for both data sets and samples were examined one-by-one by modeling one label into the Pymol structures, used as simple reference, and the position of the second label was reconstructed from the coordinates of the first label according to each solution.[26] The operation was carried out for both possible positions of the label in the

Table 1 Summary of the Euler angles[a] describing the label orientations in the RNA duplex and the α-helical peptide

Solution	RNA duplex	Peptide
Fit (variable $\Delta\nu$):		
$(\alpha_1,\beta_1,\gamma_1)(\alpha_2,\beta_2)$	(13,−32,−1)(66,−11)	(57,−82,32)(76,−67)
ξ, β'[b]	82, 43	128, 116
rmsd	0.17	0.19
ψ	—	±20°
Best sym.-rel. solutions:[c]		
$(\alpha_1,\beta_1,\gamma_1)(\alpha_2,\beta_2)$	(13,−32,−1)(−66,169)	As above
ξ, β'	98, 137	
$(\alpha_1,\beta_1,\gamma_1)(\alpha_2,\beta_2)$	(13,148,−179)(−66,169)	(57,98,148)(76,−67)
ξ, β'	98, 43	128, 64
Fit (fixed $\Delta\nu$):	—	
$(\alpha_1,\beta_1,\gamma_1)(\alpha_2,\beta_2)$	(123,37,−58)(31,13)	(75,−78,−175)(−143,−50)
ξ, β'	95, 32	138, 94
rmsd	0.12	0.28
Best sym.-rel. solutions:[d]		
$(\alpha_1,\beta_1,\gamma_1)(\alpha_2,\beta_2)$	(−57,143,−122)(−211,−167)	—
ξ, β'	85, 32	
$(\alpha_1,\beta_1,\gamma_1)(\alpha_2,\beta_2)$	(123,37,122)(−211,−167)	—
ξ, β'	85, 14	

[a] Euler angles are defined using the right-handed coordinate system for counter-clockwise rotations around z, y', z''. The primes denote the new coordinate systems generated after each rotation. [b] Definition given in the text. The following tensor principal axis values (x,y,z) were used to simulate the EPR lines: (a) RNA label: g_{xyz} = [2.0083, 2.0061, 2.0023]; A_{xyz} = [4.6, 5.0, 37] G; (b) TOPP label: g_{xyz} = [2.0101, 2.0065, 2.0023]; A_{xyz} = [6.3, 6.3, 34] G. The rmsd values were calculated over all traces of one data set. The trace with largest modulation depth was normalized to unity. [c] Symmetry-related solutions #6 and #9 from S6b (ESI) and #1 and #2 from S6d (ESI). [d] Symmetry-related solutions #11 and #14 from S6c (ESI).

sequence (S6, ESI†). Interestingly, we found that most solutions can be in principle discarded because they are not compatible with the expected structures. Four solutions were left for the RNA duplex and two for the peptide, which are reported in Table 1 and illustrated in Fig. 4. A more detailed evaluation of these solutions in terms of bio-molecular structure would require more sophisticated molecular modeling, which is beyond the scope of this work.

Conclusions

This work reports the performance of a more general experimental set up, based on variable dual frequency irradiation, to perform DEER/PELDOR at high frequencies without limitations by the difference in resonance frequency of two spin labels. Although individual aspects of the work (rigid labels, high frequency PELDOR/DEER, wideband excitation, analysis and symmetries) were discussed in the past, we demonstrate here the combination of all these features. The results show that experiments at variable frequency separation in combination with spin labels of restricted mobility supply high quality data amenable to analysis of the orientation selection in terms of bi-radical structures. Experiments at fixed frequency separation provide sufficient constraints only for bi-radicals with g axes in almost collinear arrangement. The feasibility of data analysis permitted us to recognize several symmetry-related solutions. Evaluation of these solutions is possible if information on the global molecular structure is available or additional experimental constraints are introduced.

Acknowledgements

This work has been supported by the Max Planck Society, the Deutsche Forschungsgemeinschaft (SFB 803) and the Icelandic Research Fund (090026023). We thank D. Gophane and B. Angerstein for discussions and help in sample preparation.

Notes and references

1 (*a*) A. D. Milov, A. B. Ponomarev and Yu. D. Tsvetkov, *Chem. Phys. Lett.*, 1984, **110**, 67–72; (*b*) A. D. Milov, A. G. Maryasov and Yu. D. Tsvetkov, *Appl. Magn. Reson.*, 1998, **15**, 107–143.
2 G. Jeschke, *Macromol. Rapid Commun.*, 2002, **23**, 227–246.
3 P. Borbat and J. H. Freed, *Methods Enzymol.*, 2007, **423**, 52–116.
4 O. Schiemann and T. F. Prisner, *Q. Rev. Biophys.*, 2007, **40**, 1–53.
5 S. A. Shelke and S. T. Sigurdsson, *Structural information from spin-labels and intrinsic paramagnetic centers in the biosciences, Struct. Bonding*, 2012, DOI: 10.1007/430_2011_62, in press.
6 R. G. Larsen and D. J. Singel, *J. Chem. Phys.*, 1993, **98**, 5134–5146.
7 (*a*) V. P. Denysenkov, T. F. Prisner, J. Stubbe and M. Bennati, *Proc. Natl. Acad. Sci. U. S. A.*, 2006, **103**, 13386–13390; (*b*) V. P. Denysenkov, D. Biglino, W. Lubitz, T. F. Prisner and M. Bennati, *Angew. Chem., Int. Ed.*, 2008, **47**, 1224–1227.
8 O. Schiemann, P. Cekan, D. Margraf, T. F. Prisner and S. Th. Sigurdsson, *Angew. Chem., Int. Ed.*, 2009, **48**, 3292–3295.
9 Y. Polyhach, A. Godt, C. Bauer and G. Jeschke, *J. Magn. Reson.*, 2007, **185**, 118–129.
10 A. Savitsky, A. A. Dubinskii, H. Zimmermann, W. Lubitz and K. Moebius, *J. Phys. Chem. B*, 2011, **115**, 11950–11963.
11 P. A. S. Cruickshank, D. R. Bolton, D. A. Robertson, R. I. Hunter, R. J. Wylde and G. M. Smith, *Rev. Sci. Instrum.*, 2009, **80**, 103102.
12 G. Sicoli, T. Argirević, J. Stubbe, I. Tkach and M. Bennati, *Appl. Magn. Reson.*, 2010, **37**, 539–548.
13 A. Marko, V. Denysenkoy, D. Margraf, P. Cekan, O. Schiemann, S. Th. Sigurdsson and T. F. Prisner, *J. Am. Chem. Soc.*, 2011, **133**, 13375–13379.
14 G. W. Reginsson, R. I. Hunter, P. A. S. Cruickshank, D. R. Bolton, S. Th. Sigurdsson, G. M. Smith and O. Schiemann, *J. Magn. Reson.*, 2012, **216**, 175–182.
15 (*a*) I. Kaminker, H. Yagi, T. Huber, A. Feintuch, G. Otting and D. Goldfarb, *Phys. Chem. Chem. Phys.*, 2012, **14**, 4355–4358; (*b*) I. Kaminker, I. Tkach, N. Manukovsky, Th. Huber, H. Yagi, G. Otting, M. Bennati and D. Goldfarb, *J. Magn. Reson.*, 2013, **227**, 66–71.
16 A. Marko, D. Margraf, P. Cekan, S. Th. Sigurdsson, O. Schiemann and T. F. Prisner, *Phys. Rev. E: Stat., Nonlinear, Soft Matter Phys.*, 2010, **81**, 021911.
17 J. E. Lovett, A. M. Bowen, C. R. Timmel, M. W. Jones, J. R. Dilworth, D. Caprotti, S. G. Bell, L. L. Wong and J. Harmer, *Phys. Chem. Chem. Phys.*, 2009, **11**, 6840–6848.
18 C. Abé, D. Klose, F. Dietrich, W. H. Ziegler, Y. Polyhach, G. Jeschke and H.-J. Steinhoff, *J. Magn. Reson.*, 2012, **216**, 53–61.
19 A. Marko and T. Prisner, *Phys. Chem. Chem. Phys.*, 2013, **15**, 619–627.
20 (*a*) I. Tkach, G. Sicoli, C. Höbartner and M. Bennati, *J. Magn. Reson.*, 2011, **209**, 341–346; (*b*) I. Tkach and M. Bennati, *European Pat.*, EP2486416B1, International publication Nr. WO2012/013202.
21 N. Barhate, P. Cekan, A. P. Massey and S. Th. Sigurdsson, *Angew. Chem., Int. Ed.*, 2007, **46**, 2655–2658.
22 S. Stoller, G. Sicoli, T. Y. Baranova, M. Bennati and U. Diederichsen, *Angew. Chem., Int. Ed.*, 2011, **50**, 9743–9746.
23 C. Höbartner, G. Sicoli, F. Wachowius, D. B. Gophane and S. Th. Sigurdsson, *J. Org. Chem.*, 2012, **77**, 7749–7754.
24 G. Sicoli, F. Wachowius, M. Bennati and C. Höbartner, *Angew. Chem., Int. Ed.*, 2010, **49**, 6443–6447.
25 T. E. Edwards, P. Cekan, G. W. Reginsson, S. A. Shelke, A. R. Ferré-D'Amaré, O. Schiemann and S. Th. Sigurdsson, *Nucleic Acids Res.*, 2011, **39**, 4419–4426.
26 For the modeling of the TOPP label into the peptide a DFT optimized structure of TOPP was used as reported in ref. 21.
27 K. Möbius and A. Savitsky, *High-Field EPR Spectroscopy on Proteins and their Model Systems: Characterization of Transient Paramagnetic States*, RSC Publishing, London, 2009.